

Correlation Information Bottleneck: Towards Adapting Pretrained Multimodal Models for Robust Visual Question Answering

Jingjing Jiang · Ziyi Liu · Nanning Zheng

Received: date / Accepted: date

Abstract Benefiting from large-scale pretrained vision language models (VLMs), the performance of Visual Question Answering (VQA) has approached human oracle performance. However, finetuning large-scale pretrained VLMs with limited data usually suffers from overfitting and poor generalization issues, leading to a lack of model robustness. In this paper, we aim to improve the input robustness, i.e., the ability of models to defend against visual and linguistic input variations as well as shortcut learning involved in inputs, from the perspective of Information Bottleneck when adapting pretrained VLMs to the downstream VQA task. Generally, internal representations obtained by pretrained VLMs inevitably contain irrelevant and redundant information for a specific downstream task, resulting in statistically spurious correlations and insensitivity to input variations. To encourage the obtained representations to converge to a minimal sufficient statistic in vision-language learning, we propose the Correlation Information Bottleneck (CIB) principle, which seeks a tradeoff between representation compression and redundancy by minimizing the mutual information (MI) between inputs and internal representations while maximizing the MI between outputs and the representations. Furthermore, CIB measures the internal correlations among visual and linguistic inputs and representations via a symmetrized joint MI estimation. Extensive experiments on five VQA datasets of input robustness demonstrate the effectiveness and superiority of the proposed CIB in terms of robustness and accuracy.

Keywords information bottleneck · robustness · visual question answering · vision-language model

1 Introduction

Visual Question Answering (VQA) (Antol et al., 2015) is a classical vision-language task for answering questions conditioned on understanding of a given image. Recently, the large-scale pretrained Vision-Language Models (VLMs) (Wang et al., 2022; Zeng et al., 2022; Wang et al., 2022; Yu et al., 2022; Wang et al., 2022; Li et al., 2022; Yuan et al., 2021; Wang et al., 2021) have elevated the VQA performance to the level of human oracle. However, finetuning extremely large-scale pretrained VLMs with limited data for the downstream VQA task usually suffers from overfitting and poor generalization issues, making the improvement in robustness brought by pretrained VLMs relatively limited and far less than the improvement in accuracy.

In this paper, we explore the input robustness and aim to improve the robustness when adapting pretrained VLMs to the downstream VQA task. The input robustness refers to the capability of VQA models to defend against visual variations (e.g., question-related object removal (Agarwal et al., 2020) in images), linguistic variations (e.g., word substitution and sentence rephrasing (Shah et al., 2019; Whitehead et al., 2020) in questions), and multimodal shortcut learning involved in both input images and questions (Dancette et al., 2021). Practically, in the finetuning process, VQA is usually formulated as a multi-answer classification problem or a text generation problem, in which pretrained multimodal transformers usually act as representation extractors with rich knowledge and are used to extract the vision-language representations for answer prediction. As such, improving input robustness of models essentially makes the obtained representation more compact and task-related.

To this end, we propose to improve input robustness from an information-theoretical perspective. From this view, one possible reason for poor robustness is that representations yielded by pretrained VLMs inevitably contain irrelevant

Jingjing Jiang · Ziyi Liu · Nanning Zheng
Institute of Artificial Intelligence and Robotics, Xi'an Jiaotong University, Xi'an, Shaanxi, 710049, China
E-mail: jingjingjiang2017@gmail.com

and redundant information for the specific downstream task. Specifically, the irrelevant information will encourage models to learn statistically spurious correlations between representations and labels, while task-agnostic redundant information will reduce the sensibility of models to input variations. Both the irrelevant and redundant information will impair the input robustness of models. Therefore, to obtain more robust representations when adapting pretrained VLMs to the downstream VQA, we expect models to discard irrelevant and redundant information in representations while preserving the task-relevant information. The Information Bottleneck (IB) (Tishby et al., 2000) principle can seek a tradeoff between representation compression and redundancy. Motivated by this, we exploit the IB principle to find the minimal sufficient statistic of the obtained representations for more robust VQA models.

We propose Correlation Information Bottleneck (CIB) to improve the input robustness when adapting pretrained VLMs to the downstream VQA task. Specifically, CIB promotes the vision-language representations obtained by pretrained VLMs to converge to a minimal sufficient statistic by minimizing mutual information (MI) between the representations and inputs while maximizing MI between the representations and outputs. In addition to the overall dependency between the visual and linguistic inputs and the corresponding internal representations, we utilize a symmetrized joint MI to measure the internal correlations among visual and linguistic representations and inputs, guiding VQA models to better capture the actual correlations. Furthermore, to consider different transformer architectures of pretrained VLMs (i.e., the single-stream encoder, two-stream encoder, and encoder-decoder), we unify the internal representations of different pretrained VLMs for CIB estimation using the representation after visual and linguistic embedding layers.

To demonstrate the proposed CIB principle, we first provide a rigorous theoretical derivation of the lower bound of CIB. After that, we apply CIB to finetune seven baseline pretrained VLMs (i.e., VisualBERT (Li et al., 2019), VL-BERT_B (Su et al., 2020), UNITER_B (Chen et al., 2020), LXMERT (Tan and Bansal, 2019), ViLBERT (Lu et al., 2019), VL-T5 (Cho et al., 2021), and ALBEF (Li et al., 2021)) on five VQA datasets on input robustness: VQA-Rephrasings (Shah et al., 2019), VQA P2 (Whitehead et al., 2020), IV-VQA (Agarwal et al., 2020), CV-VQA (Agarwal et al., 2020), and VQA-CE (Dancette et al., 2021). Extensive experiments consistently show that CIB can significantly improve the input robustness of baseline models with different transformer architectures and show the superiority of CIB over existing methods.

The rest of the paper is organized as follows. Section 2 introduces related literatures on robustness in VQA, information bottleneck, and vision-language models. Section 3 elaborates the proposed Correlation Information Bottleneck

(CIB) principle and the application of CIB in finetuning. In Section 4, we conduct comprehensive experiments and discussions to demonstrate the effectiveness and superiority of CIB in terms of robustness and accuracy. In Section 5, we provide the rigorous theoretical derivation of CIB.

2 Related Work

2.1 Robustness in VQA

Recently, in order to promote the practical application of VQA models, many works have been proposed to study various VQA robustness, such as input robustness (Agarwal et al., 2020; Shah et al., 2019; Whitehead et al., 2020; Kant et al., 2021), human-adversarial robustness (Li et al., 2021; Sheng et al., 2021), and the robustness against answer distribution shift (Agrawal et al., 2022; Pan et al., 2022; Kervadec et al., 2021; Jiang et al., 2021; Teney et al., 2020; Clark et al., 2019; Goyal et al., 2017). In this paper, we explore input robustness, which is the capability of VQA models to defend against visual and linguistic variations, such as rephrasing questions (Shah et al., 2019; Whitehead et al., 2020), manipulating images (Agarwal et al., 2020), and shortcut learning involved in multimodal inputs (Dancette et al., 2021). The prevailing method to improve input robustness is data augmentation, i.e., generating additional data to train more robust VQA models. While data augmentation is a feasible and effective solution, the quality of the generated data is uncontrollable (e.g., limited expressiveness and excessive verbosity), and the human-generated process is time-consuming. Besides, the cycle-consistency between the original question and its rephrasings (Shah et al., 2019), contrastive learning (Kant et al., 2021), and adversarial training (Li et al., 2020) are also introduced to improve input robustness. All recent studies demonstrate state-of-the-art VQA models are still vulnerable to input variations attacks. In this paper, we propose to further improve the input robustness of existing VQA models from an information-theoretic perspective.

2.2 Information Bottleneck

Information Bottleneck (IB) principle is originally proposed by Tishby et al. (Tishby et al., 2000) for information compression, and is later applied to analyze deep learning model architectures (Tishby and Zaslavsky, 2015; Shwartz-Ziv and Tishby, 2017). Essentially, the IB objective is to seek a tradeoff between maximizing the predictive accuracy and minimizing the representation complexity. Some recent researches target exploiting the IB principle to improve the model robustness and generalization, especially in Domain Generalization (Du et al., 2020; Li et al., 2022), OOD Generalization (Ahuja et al., 2021), Multiview Representation

Learning (Federici et al., 2020; Bao, 2021), and finetuning of Pretrained Language Models (Mahabadi et al., 2021; Wang et al., 2021). Besides, some works (Wang et al., 2022; Zhou et al., 2022; Pan et al., 2021; Jeon et al., 2021; Dubois et al., 2020) aim to learn the disentangled optimal representation from an IB perspective. Since IB can facilitate compact and meaningful representations learning, we extend it to vision-language learning and apply it to obtain robust VQA models.

2.3 Vision-Language Models

Vision-Language pretraining aims to learn task-agnostic visiolinguistic representations for improving the performance of downstream tasks in a finetuning fashion (Huang et al., 2020; Zhou et al., 2020; Shi et al., 2020; Li et al., 2021; Kim et al., 2021; Sun et al., 2021; Huang et al., 2021; Dou et al., 2022; Zhong et al., 2022). From the perspective of model architecture, prevailing pretrained vision-language models (VLMs) can be roughly grouped into three types: single-stream encoder (Su et al., 2020; Chen et al., 2020; Kim et al., 2021; Gan et al., 2020; Li et al., 2020; Zhang et al., 2021), two-stream encoder (Tan and Bansal, 2019; Lu et al., 2019, 2020; Yu et al., 2021; Li et al., 2021), and encoder-decoder (Wang et al., 2022; Li et al., 2022; Cho et al., 2021; Li et al., 2021; Zeng et al., 2022). Specifically, the single-stream models first align image regions and text tokens and then apply a uniform transformer (Vaswani et al., 2017) to learn the contextualized representations. The two-stream models first use two separate transformers to learn high-level representations of image and text, and then integrate the two modalities with a cross-modal transformer. The encoder-decoder models respectively utilize encoder and decoder to learn multimodal representations and to generate related texts for specific downstream tasks. In this paper, we unify the three typical types of pretrained VLMs models and propose CIB to improve the input robustness of models when adapting these pretrained VLMs for the downstream VQA task.

3 Methodology

In this section, we first state the preliminaries of problem setting and the general Information Bottleneck (IB) principle. Then, we introduce the proposed Correlation Information Bottleneck (CIB) and explain how CIB is applied to finetune pretrained vision-language models (VLMs).

3.1 Preliminary

3.1.1 Problem Setting

In the finetuning process, the single-stream and two-stream VLMs usually formulate the VQA task as a multi-answer

classification problem, while encoder-decoder VLMs always regards VQA as a text generation task (Wang et al., 2022; Cho et al., 2021), i.e., generating free-form textual answers for a given question instead of selecting a specific one from the predefined set of answers. Given a VQA dataset $\mathcal{D} = \{(I, Q, y) \in \mathcal{I} \times \mathcal{Q} \times \mathcal{Y}\}$, where I is an image, Q is a question, and y is an answer, VLMs take image-question pairs as input, where the image is further represented as a set of image regions or patches $\{v_1, \dots, v_K\}$ (K is the number of regions or patches in one image) and the question is tokenized as a token sequence $\{w_1, \dots, w_L\}$ (L is the number of word tokens in a question). For the single-stream and two-stream VLMs, they output the answer probability distribution Y using a additional VQA Head module, which is implemented by two fully-connected layers sandwiched with GeLU activation and Layer Normalization operation. While for the encoder-decoder VLMs, they directly generate textual answers.

3.1.2 IB View of Representation Learning

From an information-theoretical view, seeking a robust representation T for pretrained VLMs is equivalent to preserving information about the output Y while removing irrelevant and redundant information from the input X . This is because for the given VQA task, the irrelevant and redundant information may encourage pretrained VLMs to learn superfluous correlations between answer labels and inputs. Formally, the IB principle (Tishby et al., 2000; Tishby and Zaslavsky, 2015) formulates vision-language representation learning as an information-theoretic tradeoff and finds an optimal representation by maximizing the Lagrangian

$$\mathcal{L}_{\text{IB}} := I(Y; T) - \beta I(X; T), \quad (1)$$

where, $\beta \geq 0$ controls the tradeoff between compression and prediction, and $I(\cdot; \cdot)$ denotes mutual information (MI).

3.2 Correlation Information Bottleneck

In vision-language representation learning, given the two modal inputs X^v and X^l , T^v and T^l respectively denote the corresponding internal visual and linguistic representations. To extend the general IB principle to this multimodal setting, we group the input sources and internal representations as $X = [X^v, X^l]$ and $T = [T^v, T^l]$. Therefore, the training objective is to learn the minimal sufficient representation T that discards all irrelevant and redundant information from the input X for the given VQA task.

Specifically, to derive a differentiable IB estimation in vision-language representation learning, we first focus on the term $I(Y; T)$ in Eq. (1), which can be rewritten as the following form using conditional probability definition:

$$I(Y; T) = \int p(y, t) \log \frac{p(y|t)}{p(y)} dy dt. \quad (2)$$

Since the conditional probability $p(y|t)$ is intractable, we instead estimate $I(Y; T)$ with the BA (Barber and Agakov, 2003) lower bound:

$$I(Y; T) \geq \int p(y, t) \log q(y|t) dy dt - \int p(y) \log p(y) dy, \quad (3)$$

where, $q(y|t)$ is an accessible auxiliary distribution of $p(y|t)$, and $-\int p(y) \log p(y) dy = H(Y)$ is the entropy of labels, which is independent to the optimization procedure in finetuning. Ignoring $H(Y)$, the remaining term of the lower bound in Eq. (3) is equal to $-H(Y|T)$, which means that maximizing the lower bound of $I(Y; T)$ is equivalent to minimizing the cross-entropy loss of a specific task.

Next, we consider the mutual information between the input sources and their corresponding representations, that is, $I(X; T)$ in Eq. (1). In addition to measuring the overall dependency between X and T (i.e., regarding visual and linguistic representations as a whole one), we also concerns the internal correlations among multimodal inputs and representations X^v, X^l, T^v , and T^l , which can guide pretrained VLMs to learn correlations between visual and linguistic representations. Therefore, we propose to maximize the Correlation Information Bottleneck (CIB) formula:

$$\mathcal{L}_{\text{CIB}} := I(Y; T) - \beta I(X^v, X^l; T^v, T^l), \quad (4)$$

where, $I(X^v, X^l; T^v, T^l)$ can be regarded as a symmetrized variant of joint mutual information (Bennasar et al., 2015) that considers the relevance of the input set $[X^v, X^l]$ and the relevance of the representation set $[T^v, T^l]$. To efficiently approximate $I(X^v, X^l; T^v, T^l)$, we first expand it conditioned on the properties of mutual information and the data processing inequality in representation learning (Federici et al., 2020). The derivation can be formally stated by Theorem 1 (see Section 5 for proof):

Theorem 1 (Upper Bound of $I(X^v, X^l; T^v, T^l)$) *Given two groups of random variables $X = [X^v, X^l]$, $T = [T^v, T^l]$, the mutual information $I(X^v, X^l; T^v, T^l)$ can be upper-bounded with*

$$I(X; T) = I(X^v, X^l; T^v, T^l) \leq \underbrace{I(X^v; T^v)}_{\textcircled{1}} + \underbrace{I(X^l; T^l)}_{\textcircled{2}} - \underbrace{I(T^v; T^l)}_{\textcircled{3}} + \underbrace{D_{\text{SKL}}}_{\textcircled{4}}, \quad (5)$$

where, D_{SKL} denotes the Symmetric Kullback-Leibler (KL) divergence and can be obtained by averaging the divergence $D_{\text{KL}}(p(t^v|x^v)||p(t^l|x^l))$ and $D_{\text{KL}}(p(t^l|x^l)||p(t^v|x^v))$.

Afterward, we further upper-bound the MI between an input and its representation with a localized formulation of IB (Wang et al., 2021). Formally, for the visual and linguistic

inputs X^v, X^l , they are essentially two sets of random variables, $X^v = [X_1^v, X_2^v, \dots, X_K^v]$, $X^l = [X_1^l, X_2^l, \dots, X_L^l]$, f_{θ^v} and f_{θ^l} are the two functions that map X^v and X^l into visual and linguistic representations, $T^v = [T_1^v, T_2^v, \dots, T_K^v] = [f_{\theta^v}(X_1^v), f_{\theta^v}(X_2^v), \dots, f_{\theta^v}(X_K^v)]$ and $T^l = [T_1^l, T_2^l, \dots, T_L^l] = [f_{\theta^l}(X_1^l), f_{\theta^l}(X_2^l), \dots, f_{\theta^l}(X_L^l)]$. The MI between the visual (linguistic) input and the visual (linguistic) representation can be maximized by

$$I(X^v; T^v) \leq K \sum_{i=1}^K I(X_i^v; T_i^v); \quad (6)$$

$$I(X^l; T^l) \leq L \sum_{i=1}^L I(X_i^l; T_i^l). \quad (7)$$

Therefore, the lower bound of \mathcal{L}_{CIB} can be stated as the following Theorem 2.

Theorem 2 (Lower Bound of CIB) *Given two groups of random variables, $X = [X^v, X^l]$ and $T = [T^v, T^l]$, where X^v, X^l, T^v , and T^l are represented as the sets of random variables, i.e., $X^v = [X_1^v, X_2^v, \dots, X_K^v]$, $X^l = [X_1^l, X_2^l, \dots, X_L^l]$, $T^v = [T_1^v, T_2^v, \dots, T_K^v]$, and $T^l = [T_1^l, T_2^l, \dots, T_L^l]$. Two deterministic functions, f_{θ^v} and f_{θ^l} , make $T^v = [T_1^v, T_2^v, \dots, T_K^v] = [f_{\theta^v}(X_1^v), f_{\theta^v}(X_2^v), \dots, f_{\theta^v}(X_K^v)]$, $T^l = [T_1^l, T_2^l, \dots, T_L^l] = [f_{\theta^l}(X_1^l), f_{\theta^l}(X_2^l), \dots, f_{\theta^l}(X_L^l)]$. Then, Correlation Information Bottleneck (CIB) can be bounded with the following formulation*

$$\begin{aligned} \mathcal{L}_{\text{CIB}} &= I(Y; T) - \beta I(X^v, X^l; T^v, T^l) \\ &\geq I(Y; T) - \beta \left[K \sum_{i=1}^K I(X_i^v; T_i^v) + L \sum_{i=1}^L I(X_i^l; T_i^l) \right. \\ &\quad \left. - I(T^v; T^l) + D_{\text{SKL}} \right]. \end{aligned} \quad (8)$$

The theorem indicates that in vision-language representation learning, once $I(Y; T)$ is regarded as a task-related objective, $-\beta I(X^v, X^l; T^v, T^l)$ can be used to constrain the compactness and redundancy of the representations obtained by pretrained VLMs. In other words, CIB encourages models to seek more robust representations by trading off representation redundancy and compression.

3.3 Adapting Pretrained VLMs to VQA with Correlation Information Bottleneck

As shown in Figure 1(a), 1(b), and 1(c), there are three typical transformer architectures of pretrained VLMs: single-stream encoder (Li et al., 2019; Su et al., 2020; Chen et al., 2020), two-stream encoder (Tan and Bansal, 2019; Lu et al., 2019), and encoder-decoder (Cho et al., 2021; Li et al., 2021). When finetuning pretrained VLMs with CIB, to unify the three typical architectures into one formulation, as shown

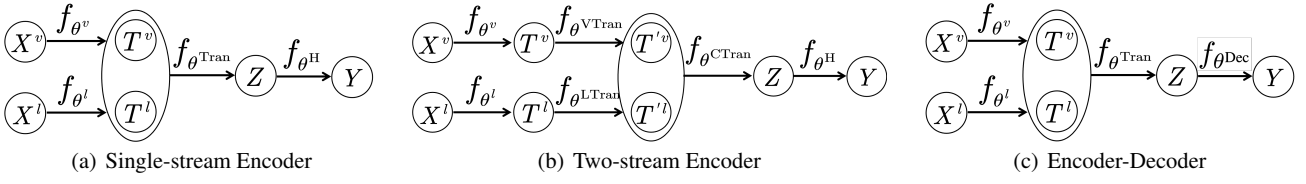


Fig. 1 The information flow of three typical transformer architectures of pretrained VLMs.

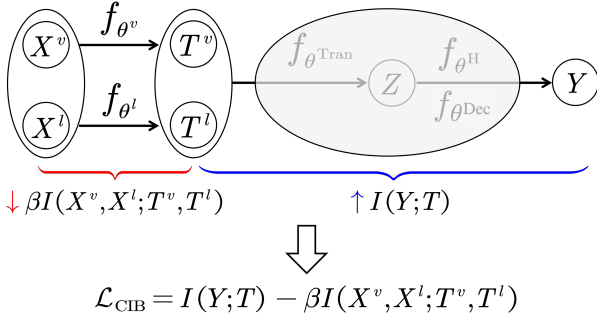


Fig. 2 Illustration of using CIB to adapt pretrained VLMs to downstream task. CIB seeks the minimal sufficient statistic by minimizing MI between inputs and the internal representations (\downarrow) while maximizing MI between outputs and the representations (\uparrow).

in Figure 2, we utilize the region-level or patch-level visual features after the visual Embedding layer (i.e., f_{θ^v} is the parametric Embedding layer) as the internal visual representation T^v . Analogously, the token-level linguistic features after the linguistic Embedding layer (f_{θ^l}) is regarded as the internal linguistic representation T^l . All the following Transformer layers ($f_{\theta^{Tran}}$) and the VQA Head module (f_{θ^H}) for the single-stream and two-stream VLMs as well as the Decoder ($f_{\theta^{Dec}}$) for the encoder-decoder VLMs serve as the parametric approximator to yield Y given $T = [T^v, T^l]$.

In summary, to utilize CIB to finetune pretrained VLMs with different transformer architectures, we regard $I(Y; T)$ in Eq. (8) as the task-related loss (i.e., the cross-entropy loss for answer prediction) and the remaining terms in Eq. (8) as a regularizer. The regularizer controls representation redundancy and improves the input robustness of models by discarding information that will encourage models to learn spurious correlations.

3.3.1 Estimating MI Terms in CIB

As stated in Theorem 2, in addition to the task-related term MI $I(Y; T)$, $I(X^v, X^l; T^v, T^l)$ can be expanded into four computable MI terms. Specifically, in the finetuning process, for sample pairs $\{(X_i^v, T_i^v)\}_{i=1}^K$ and $\{(X_i^l, T_i^l)\}_{i=1}^L$, the conditional probability distributions $p(t^v|x^v)$ and $p(t^l|x^l)$ are known. We thus adopt a sample-based differentiable MI estimator, CLUB (Cheng et al., 2020), to approximate the upper bound of MI between the visual (linguistic) inputs and its

corresponding representations, i.e.,

$$\begin{aligned}\hat{I}(X^v; T^v) &= \frac{1}{K^2} \sum_{i=1}^K \sum_{j=1}^K [\log p(t_i^v|x_i^v) - \log p(t_j^v|x_i^v)], \\ \hat{I}(X^l; T^l) &= \frac{1}{L^2} \sum_{i=1}^L \sum_{j=1}^L [\log p(t_i^l|x_i^l) - \log p(t_j^l|x_i^l)].\end{aligned}\quad (9)$$

For $I(T^v; T^l)$, it is difficult to be estimated directly due to the different sequence lengths of $T^v \in \mathbb{R}^{K \times d}$ and $T^l \in \mathbb{R}^{L \times d}$. To estimate $I(T^v; T^l)$, we first transform the sequence representations into global visual and linguistic representations, $\bar{T}^v \in \mathbb{R}^d$ and $\bar{T}^l \in \mathbb{R}^d$, using two one-layer fully-connected (FC) networks. Then, to guarantee the inequality in Eq. (8) hold, we should approximate the lower bound of $I(T^v; T^l)$. Therefore, we estimate the lower bound of it with NWJ (Poole et al., 2019), i.e.,

$$\hat{I}(\bar{T}^v; \bar{T}^l) = \mathbb{E}_{p(\bar{T}^v, \bar{T}^l)} [\log f(\bar{T}^v, \bar{T}^l)] - \frac{1}{e} \mathbb{E}_{p(\bar{T}^v)p(\bar{T}^l)} [f(\bar{T}^v, \bar{T}^l)], \quad (10)$$

where, $f(\cdot)$ is a discriminant function implemented by a two-layer FC network.

For D_{SKL} in \mathcal{L}_{CIB} , we compute the symmetric Kullback-Leibler (KL) divergence by

$$\begin{aligned}D_{SKL} &= \frac{1}{2} [D_{KL}(p(t^v|x^v)||p(t^l|x^l)) + \\ &\quad D_{KL}(p(t^l|x^l)||p(t^v|x^v))].\end{aligned}\quad (11)$$

Since $p(t^l|x^l)$ and $p(t^v|x^v)$ have a known probability density, we directly compute the two KL divergences using internal visual and linguistic representations.

4 Experiment

The goal of our experiments is to verify whether using CIB as a training objective when adapting pretrained VLMs to the downstream VQA task will make models more robust. To this end, we primarily consider the following questions: (1) Facilitated by CIB, are models more robust against input variations? (2) How does each component of CIB contribute to model robustness? (3) Why can CIB improve the input robustness of models?

Table 1 Dataset details

Datasets	Perturbation	Metric	QType	Training Dataset	Evaluation			
					len(Q)	#IQ	#PER/CE	#ORI/Easy
VQA-Rephrasings (Shah et al., 2019)	Rephrasing	CS(k)	All	VQA v2 train	7.15	162k	121,516	40,504
VQA P2 (Whitehead et al., 2020)	Par & Syn & Ant	CS(k)	All	VQA v2 train	6.32	52k	26,512	25,814
IV-VQA (Agarwal et al., 2020)	Invariant object	#flips	All	VQA v2 train	5.85	120k	83,700	36,181
CV-VQA (Agarwal et al., 2020)	Covariant object	#flips	Num	VQA v2 train	5.83	4k	4,141	2,641
VQA-CE (Dancette et al., 2021)	Counterexample	-	All	VQA v2 train	6.19	214k	63,298	147,681

Table 2 Summary of baseline pretrained VLMs

Domain	Pretrained VLMs	Architecture	Pretraining Dataset	Visual Embedding	test-dev	test-std
ID	VisualBERT (Li et al., 2019)	single-stream	COCO	Region Feature	70.80	71.00
ID+OOD	VL-T5 (Cho et al., 2021)	encoder-decoder	COCO, VG, GQA, VQA, VGQA	Region Feature	-	70.30
	LXMERT (Tan and Bansal, 2019)	two-stream	COCO, VG, GQA, VQA, VGQA	Region Feature	72.42	72.54
	UNITER _B (Chen et al., 2020)	single-stream	COCO, VG, CC, SUB	Region Feature	72.70	72.91
	ALBEF (Li et al., 2021)	encoder-decoder	COCO, VG, CC, SUB	Patch Feature	74.54	74.70
OOD	ViLBERT (Lu et al., 2019)	two-stream	CC	Region Feature	70.55	70.92
	VL-BERT _B (Su et al., 2020)	single-stream	CC	Region Feature	71.16	-

4.1 Experimental Setups

4.1.1 Datasets

To evaluate the input robustness of our methods, we conduct experiments on five datasets: VQA-Rephrasings (Shah et al., 2019), VQA P2 (Whitehead et al., 2020), IV-VQA (Agarwal et al., 2020), CV-VQA (Agarwal et al., 2020), and VQA-CE (Dancette et al., 2021). VQA-Rephrasings and VQA P2 evaluate the robustness against linguistic variations, IV-VQA and CV-VQA evaluate the robustness against visual variations, and VQA-CE evaluates the robustness against shortcut learning involving inputs. Table 1 summarizes the dataset details, including the type of perturbation, the specific evaluation metrics for robustness, the type of question (QType), the shared training dataset, and statistics of test dataset. Since all datasets are built on VQA v2 (Goyal et al., 2017) val split, we thus only train our models on VQA v2 training set.

The statistics involve the number of total image-question pairs (#IQ), perturbation samples (#PER/CE), and original samples (#ORI/Easy), as well as the average question length (len(Q)). Specifically, **VQA-Rephrasings** averagely collects 3 rephrasings for each of 40,504 questions sampled from the val set of VQA v2, and obtains about 162k image-question pairs. **VQA P2** creates three types of linguistic perturbations, i.e., sentence rephrasing (Par) and word substitution with Synonym (Syn) and Antonym (Ant), for 25,814 sampled questions, and finally obtains about 52k image-question pairs. **IV-VQA** is created using a GAN-based resynthesis technique to remove objects irrelevant to the image-question pairs from the image (i.e., the removal of objects does not lead to any change for the answer). Conversely, **CV-VQA**

targets counting questions (Num) and removes one relevant object that makes the answer prediction on the quantity of such objects are expected to be subtracted by 1. Finally, IV-VQA and CV-VQA have about 120k and 4k image-question pairs, respectively. **VQA-CE** is an evaluation protocol for multimodal shortcuts involved in images and questions. It leverages the detected shortcuts on training set to obtain 63,298 counterexamples, in which all shortcuts provide an incorrect answer, from VQA v2 val set. In addition, VQA-CE builds 147,681 easy examples on which at least one shortcut provides the correct answer.

4.1.2 Evaluation Metrics

We adopt the standard evaluation protocol from previous work (Antol et al., 2015) and evaluate the performance of our methods with VQA-Score. In addition, we follow the work (Shah et al., 2019) to evaluate the robustness against **linguistic variations** using Consensus Score, which is the ratio of the number of subsets where all questions are answered correctly to the total number of subsets of size k . Specifically, for each question group Q with one original question and corresponding n rephrasings of the question, all subsets with size k are nC_k , then Consensus Score can be defined as

$$CS(k) = \sum_{q \in Q', Q' \subset Q, |Q'| = k} \frac{\mathbb{1}_{\Theta}(q)}{{}^nC_k}, \quad (12)$$

where, Θ is a set where the answer of question q is correct, and $\mathbb{1}$ is an indicator function defined on Θ . Obviously, the higher the average Consensus Score at higher values of k , the more robust the model is. To evaluate the robustness against **visual variations**, we follow Agarwal et al. (Agarwal et al.,

Table 3 Results of robustness against linguistic variations (i.e., sentence rephrasing) on the VQA-Rephrasings (Shah et al., 2019) dataset

Methods	VQA-Score		Robustness Metric			
	PER	ORI	CS(1)	CS(2)	CS(3)	CS(4)
<i>Data Augmentation</i>						
BUTD (Anderson et al., 2018)	51.22	61.51	60.55	46.96	40.54	34.47
+ CC (Shah et al., 2019)	52.58 (+1.36)	62.44 (+0.93)	61.66 (+1.11)	50.79 (+3.83)	44.68 (+4.14)	42.55 (+8.08)
Pythia (Jiang et al., 2018)	54.20	64.08	63.43	52.03	45.94	39.49
+ CC (Shah et al., 2019)	55.65 (+1.45)	64.52 (+0.44)	64.36 (+0.93)	55.45 (+3.42)	50.92 (+4.98)	44.30 (+4.81)
BAN (Kim et al., 2018)	55.87	64.97	64.88	53.08	47.45	39.87
+ CC (Shah et al., 2019)	56.59 (+0.72)	65.87 (+0.90)	65.77 (+0.89)	56.94 (+3.86)	51.76 (+4.31)	48.18 (+8.31)
MMT (Kant et al., 2021)	-	-	67.58	60.04	55.53	52.36
ConClaT (Kant et al., 2021)	-	-	68.62 (+1.04)	61.42 (+1.38)	57.08 (+1.55)	53.99 (+1.63)
<i>w/o Data Augmentation</i>						
UNITER _B (Chen et al., 2020)	-	-	71.29	63.95	59.48	56.31
MANGO _B (Li et al., 2020)	-	-	72.66 (+1.37)	66.03 (+2.08)	61.92 (+2.44)	58.95 (+2.64)
VILLA _B (Gan et al., 2020)	-	-	72.18	65.28	60.99	57.93
MANGO _{VB} (Li et al., 2020)	-	-	72.78 (+0.60)	65.97 (+0.69)	61.70 (+0.71)	58.59 (+0.66)
VisualBERT (Li et al., 2019) [†]	62.03	68.46	70.44	62.84	58.41	55.06
+ Our CIB	63.10 (+1.07)	69.78 (+1.32)	71.85 (+1.41)	64.16 (+1.32)	59.54 (+1.13)	56.31 (+1.25)
VL-T5 (Cho et al., 2021) [†]	65.64	-	71.78	65.35	62.68	61.00
+ Our CIB	66.93 (+1.29)	-	73.65 (+1.87)	67.48 (+2.13)	64.48 (+1.80)	62.53 (+1.53)
LXMERT (Tan and Bansal, 2019) [†]	70.41	-	79.73	72.93	68.49	65.21
+ Our CIB	72.62 (+2.21)	-	82.01 (+2.28)	75.46 (+2.53)	71.05 (+2.56)	67.71 (+2.50)
UNITER _B (Chen et al., 2020) [†]	62.68	70.05	71.45	63.72	59.01	55.66
+ Our CIB	64.45 (+1.77)	70.91 (+0.86)	73.18 (+1.73)	66.21 (+2.49)	61.88 (+2.87)	58.75 (+3.09)
ALBEF (Li et al., 2021) [†]	65.66	71.13	70.89	65.52	61.74	60.14
+ Our CIB	68.00 (+2.34)	72.43 (+1.30)	73.71 (+2.82)	67.50 (+1.98)	63.60 (+1.86)	61.72 (+1.58)
ViLBERT (Lu et al., 2019) [†]	59.16	67.65	68.00	59.65	54.68	51.22
+ Our CIB	62.28 (+3.12)	69.15 (+1.50)	71.05 (+3.05)	63.54 (+3.89)	59.04 (+4.36)	55.89 (+4.67)
VL-BERT _B (Su et al., 2020) [†]	59.89	67.14	67.95	60.11	55.34	52.99
+ Our CIB	60.86 (+0.97)	68.74 (+1.60)	70.52 (+2.57)	63.46 (+3.35)	58.75 (+3.41)	53.89 (+0.90)

2020) and use #flips as the evaluation metric. The #flips is the ratio of the number of predictions mismatched before and after visual content manipulation to the total number of all samples. More concretely, on IV-VQA, if predicted answers of the original image and its corresponding edited image are different, the prediction is regarded as “flipped”. On CV-VQA, an answer on an edited image is considered to be “flipped” if it is not one less than the prediction on original image.

4.1.3 Baseline Pretrained VLMs

In this work, we consider three typical architectures of VLMs, i.e., single-stream encoder (VisualBERT (Li et al., 2019), VL-BERT_B (Su et al., 2020), and UNITER_B (Chen et al., 2020)), two-stream encoder (LXMERT (Tan and Bansal, 2019) and ViLBERT (Lu et al., 2019)), and encoder-decoder (VL-T5 (Cho et al., 2021) and ALBEF (Li et al., 2021)). When adapting to the downstream VQA task, VisualBERT, VL-BERT_B, UNITER_B, LXMERT, and ViLBERT formulate VQA as a multi-answer classification problem. While VL-T5 and ALBEF regard VQA as a text generation task.

Table 2 summarizes details of the used pretrained VLMs. Specifically, we list their architectures, pretraining datasets,

the visual embedding (i.e., the region feature extracted by a pretrained object detector and the patch feature obtained with a linear projection), and the performance on VQA v2. Pre-training datasets include MS COCO caption (COCO) (Chen et al., 2015), Visual Genome (VG) (Krishna et al., 2017), VQA v2 (VQA) (Goyal et al., 2017), GQA balance version (GQA) (Hudson and Manning, 2019), VG-QA (VGQA) (Zhu et al., 2016), Conceptual captions (CC) (Sharma et al., 2018), and SBU captions (SBU) (Ordonez et al., 2011). In addition, since the images of VQA are derived from COCO, we follow the works (Chen et al., 2020) to divide these pre-trained VLMs into ID (in-domain), ID+OOD (in-domain + out-domain), and OOD (out-domain) according to whether they use the COCO dataset in the pretraining process.

4.1.4 Implementation Details

In all following experiments, the region feature is extracted using bottom-up attention Faster R-CNN (Anderson et al., 2018) pre-trained on Visual Genome (Krishna et al., 2017). For all baseline pretrained VLMs, the number of word tokens L is set as 20. The number of image regions K for LXMERT, VL-T5, and VisualBERT are 36, 36, and 100, respectively. For UNITER_B, ViLBERT, and VL-BERT_B, K is not fixed.

For ALBEF, K is 900. The dimension d of representation is 768. All experiments are implemented using PyTorch on one NVIDIA GTX2080Ti 12GB GPU. As for optimization, we utilize AdamW optimizer with a linear warmup with linear decay, a warmup step of 1000, a batch size of 64, and a peak learning rate of $2e-5$. The total number of training epochs is 10. The best model is selected based on the VQA-Score on a mini-split of VQA v2 train set that does not include image-question pairs when evaluating input robustness.

4.2 Input Robustness Evaluation

4.2.1 Robustness against Linguistic Variations

To evaluate the effectiveness of CIB against linguistic variations, we finetune seven baseline pretrained VLMs using CIB as an additional training objective on VQA v2 train split, and report results on VQA-Rephrasings and VQA P2. Table 3 and Table 4 respectively show the comparisons with existing methods in terms of the VQA-Score as well as $CS(k)$.

Result on VQA-Rephrasings.¹ For VQA-Rephrasings, we compare the proposed CIB with existing methods: CC (Shah et al., 2019), ConClaT (Kant et al., 2021), and MANGO (Li et al., 2020). Specifically, both CC and ConClaT augment training datasets online by training a question generation model to generate paraphrases of questions. To leverage augmented data more effectively and improve model robustness to linguistic variations, CC considers cycle consistency between the question and its rephrasings, while ConClaT jointly optimizes contrastive and cross-entropy losses. CC uses three baseline VQA models (i.e., BUTD (Anderson et al., 2018), Pythia (Jiang et al., 2018), and BAN (Kim et al., 2018)). ConClaT uses MMT (Kant et al., 2021), a modified version of UNITER, as baseline. MANGO considers pretrained VLMs (i.e., UNITER (Chen et al., 2020) and VILLA (Gan et al., 2020)) as baselines and adopts adversarial training to enhance model robustness.

As shown in Table 3, the results on seven pretrained VLMs consistently show that compared to baselines (i.e., finetuning pretrained VLMs with only the task-related cross-entropy loss for answer prediction[†]), using our CIB as an additional regularizer to train VQA models can significantly improve their robustness to linguistic variations. Therefore, it is feasible to encourage pretrained VLMs to learn more compact and robust representations from an information-theoretic perspective. Compared with state-of-the-art methods, adapting LXMERT with our CIB achieves the best performance on all metrics. In addition, we find that the data augmentation-based method (CC) brings greater improvements in the metric

¹ Considering that during pretraining, VL-T5 and LXMERT partially utilize examples from the VQA v2 validation set in the pretraining VQA task, resulting in an unreliable VQA-Score for original examples (ORI), we thus do not report the VQA-Score for ORI.

Table 4 Results of robustness against linguistic variations (i.e., sentence rephrasing, and word substitution with synonym and antonym) on the VQA P2 (Whitehead et al., 2020) dataset

Methods	PER	CS(2)
<i>Data Augmentation</i>		
StackNMN (Hu et al., 2018)	63.30	66.20
+ Q3R (Whitehead et al., 2020)	66.90 (+3.30)	72.20 (+6.00)
HybridNet (Whitehead et al., 2020)	63.30	66.60
+ Q3R (Whitehead et al., 2020)	67.00 (+4.00)	72.50 (+5.90)
XNM (Shi et al., 2019)	64.70	68.80
+ Q3R (Whitehead et al., 2020)	68.10 (+3.40)	74.40 (+5.60)
<i>w/o Data Augmentation</i>		
VisualBERT (Li et al., 2019) [†]	68.23	72.34
+ Our CIB	69.92 (+1.69)	73.83 (+1.49)
VL-T5 (Cho et al., 2021) [†]	71.63	77.34
+ Our CIB	73.47 (+1.84)	78.99 (+1.65)
LXMERT (Tan and Bansal, 2019) [†]	77.30	82.96
+ Our CIB	78.93 (+1.63)	85.07 (+2.11)
UNITER _B (Chen et al., 2020) [†]	70.36	74.36
+ Our CIB	71.30 (+0.94)	75.91 (+1.55)
ALBEF (Li et al., 2021) [†]	71.36	76.00
+ Our CIB	72.84 (+1.48)	77.46 (+1.46)
ViLBERT (Lu et al., 2019) [†]	67.18	71.39
+ Our CIB	69.92 (+2.74)	73.98 (+2.59)
VL-BERT _B (Su et al., 2020) [†]	68.36	72.52
+ Our CIB	69.82 (+1.46)	73.88 (+1.36)

of $CS(4)$. However, without data augmentation, the average improvement of our method is more significant.

Result on VQA P2. We next compare our methods with existing method Q3R (Whitehead et al., 2020) on VQA P2. Q3R arguments training data by creating linguistic variations (i.e., synonymous, paraphrastic, and antonymous) of input questions and regularizes visual reasoning process between the question and its generated questions. Q3R utilizes three baseline models: StackNMN (Hu et al., 2018), HybridNet (Whitehead et al., 2020), and XNM (Shi et al., 2019). From the results in Table 4, we can observe that finetuning pretrained VLMs with the proposed CIB can also markedly improve their robustness against question variations on VQA P2, demonstrating the effectiveness of CIB. Moreover, finetuning LXMERT with CIB achieves the best performance on VQA P2. In addition, the data augmentation-based method (Q3R) still exhibits superiority in improving the robustness of baseline VQA models.

4.2.2 Robustness against Visual Variations

We evaluate the robustness of CIB against visual variations on IV-VQA and CV-VQA using seven baseline pretrained VLMs. Table 5 shows the comparisons with existing methods in the metrics of VQA-Score as well as #flips. CL (a simple CNN+LSTM model) (Lu et al., 2015), SNMN (an attention-based method) (Hu et al., 2018), and SAAA (a compositional model) (Kazemi and Elqursh, 2017) are benchmarked by

Table 5 Results of robustness against visual variations on IV-VQA and CV-VQA (Agarwal et al., 2020)

Methods	IV-VQA			CV-VQA		
	PER	ORI	#flips ↓	PER	ORI	#flips ↓
CL (Lu et al., 2015)	-	60.21	17.89	-	39.38	81.41
SNMN (Hu et al., 2018)	-	66.04	6.52	-	47.95	78.92
SAAA (Kazemi and Elqursh, 2017)	-	70.26	7.85	-	49.90	78.44
UNITER _B (Chen et al., 2020)	-	-	8.47	-	-	40.67
MANGO _B (Li et al., 2020)	-	-	7.32 (+1.15)	-	-	38.11 (+2.56)
VILLAB (Gan et al., 2020)	-	-	7.07	-	-	38.28
MANGOV _B (Li et al., 2020)	-	-	7.43 (+0.36)	-	-	38.25 (-0.03)
VisualBERT (Li et al., 2019) [†]	46.04	81.99	26.84	30.48	76.30	30.13
+ Our CIB	47.81 (+1.77)	83.48 (+1.49)	23.91 (+2.93)	32.46 (+1.98)	77.09 (+0.79)	27.98 (+2.15)
VL-T5 (Cho et al., 2021) [†]	75.73	-	9.76	35.09	-	33.43
+ Our CIB	76.46 (+0.73)	-	8.55 (+1.21)	42.55 (+7.46)	-	30.42 (+3.01)
LXMERT (Tan and Bansal, 2019) [†]	77.83	-	12.67	38.86	-	32.80
+ Our CIB	78.57 (+0.74)	-	11.64 (+1.03)	40.47 (+1.61)	-	30.37 (+2.43)
UNITER _B (Chen et al., 2020) [†]	75.71	84.56	11.77	42.60	78.27	29.67
+ Our CIB	76.63 (+0.92)	86.05 (+1.49)	9.80 (+1.97)	46.92 (+4.32)	79.89 (+1.62)	27.99 (+1.68)
ALBEF (Li et al., 2021) [†]	86.32	93.37	8.97	50.40	93.02	28.71
+ Our CIB	87.85 (+1.53)	94.60 (+1.23)	6.37 (+2.60)	52.21 (+1.81)	94.90 (+1.88)	25.76 (+2.95)
ViLBERT (Lu et al., 2019) [†]	72.37	81.73	11.98	32.24	70.70	35.43
+ Our CIB	74.67 (+2.30)	83.35 (+1.62)	10.85 (+1.13)	35.33 (+3.09)	71.11 (+0.41)	34.01 (+1.42)
VL-BERT _B (Su et al., 2020) [†]	72.42	82.35	12.58	33.52	71.00	34.28
+ Our CIB	73.66 (+1.24)	83.37 (+1.02)	11.00 (+1.58)	35.29 (+1.77)	72.70 (+1.70)	32.09 (+2.19)

Agarwal et al. (Agarwal et al., 2020). MANGO exploits adversarial training to improve the robustness of pretrained VLMs (UNITER (Chen et al., 2020) and VILLA (Gan et al., 2020)) against visual variations. From the results in Table 5, we observe that significant improvements are achieved in all metrics across all baselines on both IV-VQA and CV-VQA, suggesting the effectiveness of CIB in improving the robustness of pretrained VLMs against visual variations. Compared with existing methods, finetuning ALBEF with CIB consistently achieves the best performance.

4.2.3 Robustness against Multimodal Shortcut Learning

To demonstrate the ability of CIB to defend against multimodal shortcuts involved in input images and questions, we conduct experiments with different pretrained VLMs on VQA-CE and compare our methods with existing methods. Results are summarized in Table 6. The compared methods in the table can be broadly classified into groups: (i) plain models (SAN (Yang et al., 2016), BLOCK (Ben-Younes et al., 2019), ViLBERT (Lu et al., 2019), and BUTD (Anderson et al., 2018)), (ii) bias-reduction methods (RUBi (Cadene et al., 2019), LMH + RMFE (Gat et al., 2020), ESR (Shrestha et al., 2020), LMH (Clark et al., 2019), LfF (Nam et al., 2020), LMH + CSS (Chen et al., 2020), and RandImg (Teney et al., 2020)). These experimental results are cited from the work (Dancette et al., 2021). As shown in Table 6, finetuning baseline pretrained VLMs with our CIB achieves significant improvements, which outperforms bias-reduction methods by a large margin, especially on counterexamples (with av-

erage improvement of 2.25). This results suggest that the proposed CIB served as a regularizer can better alleviate the spurious correlations between representations and the shortcut learning involved in multimodal inputs.

4.3 Ablation Study

In this section, we utilize UNITER_B (Chen et al., 2020), LXMERT (Tan and Bansal, 2019), and ALBEF (Li et al., 2021) as representatives of the baseline pretrained VLMs, and conduct all ablated experiments on VQA-Rephrasings (Shah et al., 2019) dataset.

4.3.1 Ablation Study on CIB Components

In CIB, $I(X^v, X^l; T^v, T^l)$ is regarded as a regularizer that is utilized to constrain representation compactness and to seek for more robust representations. As stated in Theorem 1, the upper bound of $I(X^v, X^l; T^v, T^l)$ is composed of four components: ① $I(X^v; T^v)$, ② $I(X^l; T^l)$, ③ $-I(T^v; T^l)$, and ④ D_{SKL} . To analyze how different components contribute to CIB, we perform ablation study on different meaningful combinations of these terms (i.e., other provable upper bound of $I(X^v, X^l; T^v, T^l)$). Specifically, the upper bound of the regularizer has three other meaningful combinations: $\blacktriangleright \frac{3}{2} [I(X^v; T^v) + I(X^l; T^l)]$ (i.e., ① + ②), $\blacktriangleright -I(T^v; T^l) + D_{SKL}$ (i.e., ③ + ④), and $\blacktriangleright I(X^v; T^v) + I(X^l; T^l) + D_{SKL}$ (i.e., ① + ② + ④). (See Section 5.2 for the proofs.) Table 7 shows the performance on VQA-Rephrasings. Overall, the

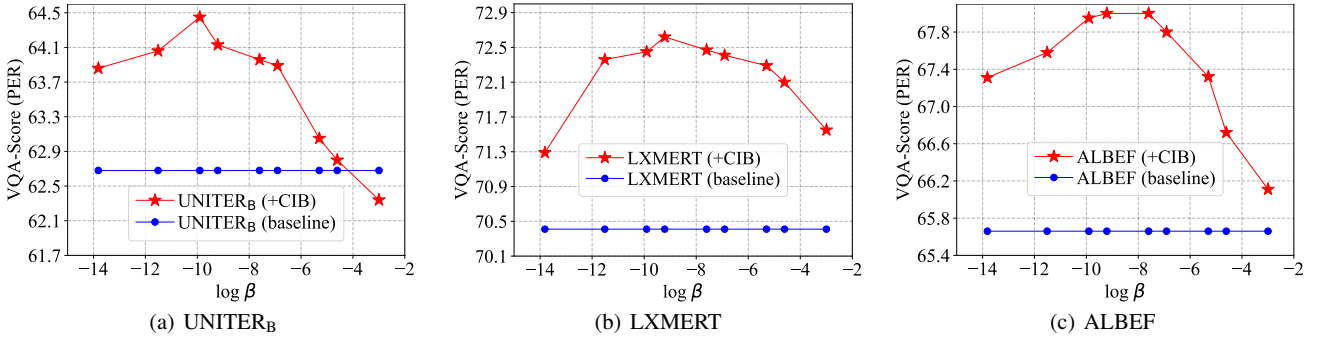


Fig. 3 The variation curve of the VQA-Score (PER) on VQA-Rephrasings (Shah et al., 2019) as $\log \beta$ increases.

Table 6 Results of robustness against multimodal shortcut learning on the VQA-CE (Dancette et al., 2021) dataset

Methods	VQA-Score	
	CE	Easy
Shortcuts (Dancette et al., 2021)	0.00	61.13
SAN (Yang et al., 2016)	26.64	68.45
BLOCK (Ben-Younes et al., 2019)	32.91	77.65
VilBERT (Lu et al., 2019)	39.24	80.50
BUTD (Anderson et al., 2018)	33.91	76.69
+ RUBi (Cadene et al., 2019)	32.25 (-1.66)	75.03 (-1.66)
+ LMH + RMFE (Gat et al., 2020)	33.14 (-0.77)	73.32 (-3.37)
+ ESR (Shrestha et al., 2020)	33.26 (-0.65)	76.18 (-0.51)
+ LMH (Clark et al., 2019)	34.26 (+0.35)	73.12 (-3.57)
+ LfF (Nam et al., 2020)	34.27 (+0.36)	76.60 (-0.09)
+ LMH + CSS (Chen et al., 2020)	34.36 (+0.45)	62.08 (-14.61)
+ RandImg (Teney et al., 2020)	34.41 (+0.50)	76.21 (-0.48)
VisualBERT (Li et al., 2019) [†]	38.75	79.42
+ Our CIB	40.86 (+2.11)	81.25 (+1.83)
VL-T5 (Cho et al., 2021) [†]	45.41	86.05
+ Our CIB	47.60 (+2.19)	88.00 (+1.95)
LXMERT (Tan and Bansal, 2019) [†]	53.61	87.63
+ Our CIB	57.14 (+3.53)	89.21 (+1.68)
UNITER _B (Chen et al., 2020) [†]	40.64	81.75
+ Our CIB	42.03 (+1.39)	82.48 (+0.73)
ALBEF (Li et al., 2021) [†]	45.39	83.88
+ Our CIB	47.87 (+2.48)	86.00 (+2.12)
VilBERT (Lu et al., 2019) [†]	38.91	80.96
+ Our CIB	41.24 (+2.33)	82.96 (+2.00)
VL-BERT _B (Su et al., 2020) [†]	36.56	80.66
+ Our CIB	38.24 (+1.68)	82.00 (+1.34)

ablation on different bounds is consistent, that is, CIB with any meaningful upper bounds can markedly improve the performance of baseline pretrained VLMs. However, CIB using our derived upper bound performs best, which empirically demonstrates that the bound in Theorem 1 is a more tight and precise bound of $I(X^v, X^l; T^v, T^l)$.

4.3.2 Ablation Study on MI Estimator

Practically, any sample-based upper bound estimator of MI can be utilized to approximate $I(X^v; T^v)$ and $I(X^l; T^l)$, and any differentiable MI lower bound estimator can be ap-

Table 7 Ablation study on the impact of different components in CIB

VLMs	CIB Terms				VQA-Score
	①	②	③	④	PER
LXMERT (Tan and Bansal, 2019)	w/o CIB				70.41
	✓	✓			72.17
			✓	✓	72.07
	✓	✓	✓	✓	72.28
UNITER _B (Chen et al., 2020)	w/o CIB				62.68
	✓	✓			64.07
			✓	✓	64.11
	✓	✓	✓	✓	63.23
ALBEF (Li et al., 2021)	w/o CIB				65.66
	✓	✓			67.11
			✓	✓	67.00
	✓	✓	✓	✓	68.00

Table 8 Ablation study on the impact of different MI estimators

VLMs	MI Estimator		VQA-Score
	Upper Bound	Lower Bound	PER
UNITER _B (Chen et al., 2020)	w/o CIB		62.68
	L1Out	NWJ	64.27
	CLUB	InfoNCE	64.14
	CLUB	MINE	64.32
LXMERT (Tan and Bansal, 2019)	w/o CIB		70.41
	L1Out	NWJ	72.31
	CLUB	InfoNCE	72.34
	CLUB	MINE	72.48
ALBEF (Li et al., 2021)	w/o CIB		65.66
	L1Out	NWJ	67.68
	CLUB	InfoNCE	68.00
	CLUB	MINE	67.91
	CLUB	NWJ	68.00

plied to approach to $I(T^v; T^l)$. To analyze the impact of different MI estimators on CIB, we consider the following

Table 9 Analysis of the impact of different internal representations obtained by the two-stream pretrained VLMs

VLMs	\mathcal{L}_{CIB}	PER
LXMERT (Tan and Bansal, 2019)	w/o CIB	70.41
	$I(Y; T) - \beta I(X^v, X^l; T'^v, T'^l)$	72.53
	$I(Y; T) - \beta I(X^v, X^l; T^v, T^l)$	72.62
ViLBERT (Lu et al., 2019)	w/o CIB	59.16
	$I(Y; T) - \beta I(X^v, X^l; T'^v, T'^l)$	62.23
	$I(Y; T) - \beta I(X^v, X^l; T^v, T^l)$	62.28

settings: (i) we alternately utilize L1Out (Poole et al., 2019) instead of CLUB (Cheng et al., 2020) as the estimator of MI upper bound to approximate $I(X^v; T^v)$ and $I(X^l; T^l)$. (ii) we approximate $I(T^v; T^l)$ with the other three estimators of MI lower bound, i.e., InfoNCE (Oord et al., 2018), NWJ (Nguyen et al., 2010), and MINE (Belghazi et al., 2018). Table 8 shows the ablated results of different MI estimators, which consistently demonstrates that CIB can effectively improve the performance of baselines with different transformer architectures and the effectiveness of CIB does not depend on a specific MI estimator.

4.4 Parameter Analysis

When using CIB to adapt pretrained VLMs to a downstream task, β controls the tradeoff between representation redundancy and compression, which is the key hyperparameter. We thus perform a grid search for β . Specifically, we consider the following values: $\beta \in [1 \times 10^{-6}, 1 \times 10^{-5}, 5 \times 10^{-5}, 1 \times 10^{-4}, 5 \times 10^{-4}, 1 \times 10^{-3}, 5 \times 10^{-3}, 1 \times 10^{-2}, 5 \times 10^{-2}]$. Figure 3 shows the variation curve of VQA-Score (PER) on the VQA-Rephrasings (Shah et al., 2019) dataset with increasing $\log \beta$. We observe that the performance starts to boost when β is a quite small value, indicating the effectiveness of CIB in improving the performance of baseline pretrained VLMs. When β increases to 5×10^{-5} , 1×10^{-4} , and 1×10^{-4} , UNITER_B, LXMERT, and ALBEF achieve the best performance, respectively. After that, the performance usually starts to drop, meaning that extremely compressed representations of pretrained VLMs may begin to compromise model performance.

4.5 Discussion

4.5.1 Why Can CIB Improve the Robustness of Baseline Pretrained VLMs?

In this section, we use LXMERT (Tan and Bansal, 2019) as a representative of the baseline pretrained VLMs, and conduct the following experiments to investigate the possible reason. More concretely, we first enumerate the image-

Table 10 Results of the effectiveness of CIB for standard VQA on VQA v2 test-dev (Antol et al., 2015)

VLMs	VQA-Score	
	Baseline	+ CIB
VisualBERT (Li et al., 2019)	70.80 (70.46 [†])	71.62 (+1.16)
VL-T5 (Cho et al., 2021)	- (70.23 [†])	71.14 (+0.91)
LXMERT (Tan and Bansal, 2019)	72.42 (72.58 [†])	72.99 (+0.41)
UNITER _B (Chen et al., 2020)	72.70 (71.63 [†])	72.11 (+0.48)
ALBEF (Li et al., 2021)	74.54 (74.54 [†])	76.27 (+1.73)
ViLBERT (Lu et al., 2019)	70.55 (70.55 [†])	71.00 (+0.45)
VL-BERT _B (Su et al., 2020)	71.16 (71.20 [†])	71.59 (+0.39)

Table 11 Results on the RefCOCO+ (Yu et al., 2016) dataset for weakly-supervised visual grounding

Methods	Val	TestA	TestB
ARN (Liu et al., 2019)	32.78	34.35	32.13
CCL (Zhang et al., 2020)	34.29	36.91	33.56
ALBEF _{itc} (Li et al., 2021)	51.58	60.09	40.19
ALBEF _{itm} (Li et al., 2021)	58.46	65.89	46.25
+ Our CIB	59.41	67.39	47.18

question pairs, whose answers are correctly predicted by the LXMERT finetuned with CIB but incorrectly predicted by the baseline LXMERT finetuned without CIB, from the VQA-Rephrasings (Shah et al., 2019) dataset. Then, we compute the attention score between the final representation $Z \in \mathbb{R}^d$ used for answer prediction and the input visual representation $X^v \in \mathbb{R}^{K \times d}$ of object regions via the formula, i.e., $\text{score}_{\text{att}} = \text{softmax}(Z \cdot (X^v)^T / \sqrt{d})$. Finally, we utilize the magenta and green color to highlight the top two objects with the highest attention scores in the image.

From the results in Figure 4, we observe that compared with the baseline LXMERT, the attended two objects obtained by the LXMERT finetuned with CIB are more consistent and question-related. This observation qualitatively illustrates that using CIB as a training objective to finetune pretrained VLMs can encourage models to learn more discriminative representations for different answers and reduce the irrelevant information to questions.

4.5.2 How Internal Representations Affect CIB?

As shown in Figure 1(b), for the pretrained VLMs with two-stream encoder (e.g., LXMERT and ViLBERT), there is an alternative to the obtained internal representations, i.e., $T = [T'^v, T'^l]$, the visual and linguistic representations after the Vision-Transformer layers ($f_{\theta^{\text{VTran}}}$) and Language-Transformer layers ($f_{\theta^{\text{LTran}}}$). When finetuning the two-stream pretrained VLMs with CIB, to analyze the impact of different internal representations, we replace the original $T = [T^v, T^l]$ in \mathcal{L}_{CIB} with $T = [T'^v, T'^l]$.

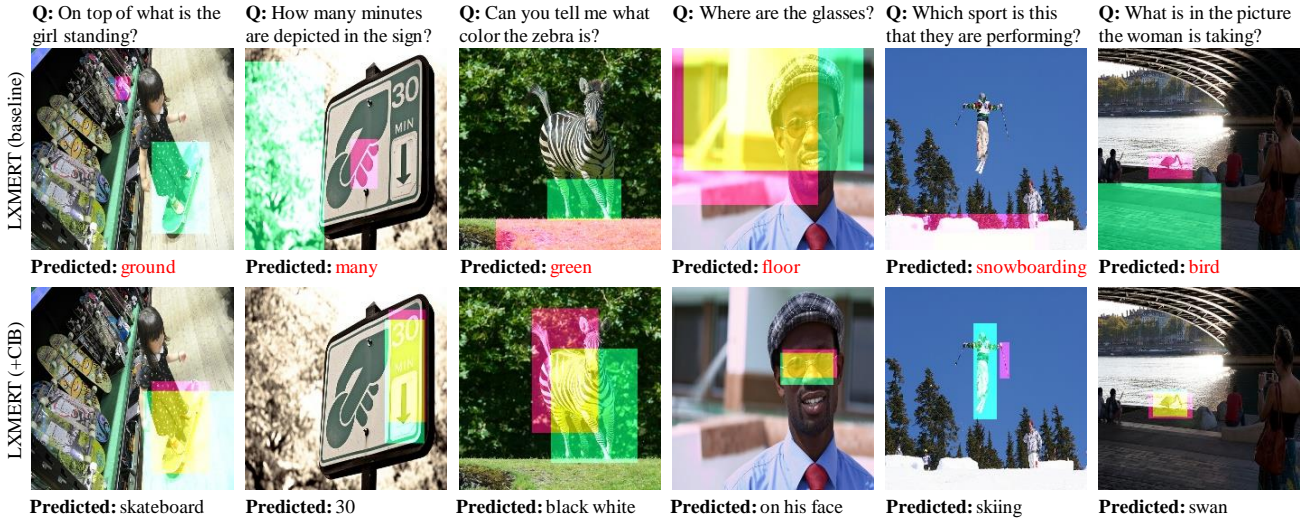


Fig. 4 Visualization of the top two objects with the highest attention scores. The image-question pairs originate from VQA-Rephrasings (Shah et al., 2019). Objects with the best and second attention scores are marked in magenta and green. The wrongly predicted answers are marked in red.

From the results in Table 9, we find that different internal representations have a slight impact on the performance of CIB, which indicates that for two-stream pretrained VLMs, using the visual and linguistic representations after the Vision and Language Transformer layers as the internal representations to estimate the MI terms in \mathcal{L}_{CIB} is also feasible.

4.5.3 How CIB Affect Standard VQA Performance?

To analyze the impact of CIB on the standard VQA performance (i.e., whether the compression of the representations obtained by pretrained VLMs impairs the standard VQA performance), we utilize CIB as the objective to train the aforementioned baseline pretrained VLMs on the VQA v2 (Goyal et al., 2017) training and validation sets. The results on VQA v2 test-dev are shown in Table 10. Since we do not use the additional question-answer pairs from Visual Genome (Krishna et al., 2017) like UNITER_B (Chen et al., 2020) for data augmentation in our experiments and some other detail differences, there are minor differences between our re-implementation[†] of baseline pretrained VLMs and the public results in original papers.

Overall, training baseline pretrained VLMs with the proposed CIB can slightly improve the standard VQA performance. In particular, the performance improvement of VisualBERT and ALBEF is relatively significant. This is due to that their visual inputs have more redundant information, such as image background and visual content irrelevant to the given question (VisualBERT and ALBEF respectively use 100 region-level features and 900 patch-level features as visual input). Therefore, our hypothesis is that a certain degree of compression of representations can reduce the redundant information learned from inputs and make the obtained representations more compact and robust.

4.5.4 Generalizability to Other Multimodal Task

To evaluate the effectiveness of CIB to other multimodal task, we consider the weakly-supervised visual grounding. Following the original experimental setups of ALBEF (Li et al., 2021), we finetune pretrained ALBEF with CIB on the RefCOCO+ (Yu et al., 2016) training dataset in a weakly-supervised setups. From the results in Table 11, we find that using CIB can further improve the performance of baseline ALBEF_{itm}, demonstrating that the proposed CIB can be effectively applied to other multimodal task.

5 Proof

5.1 Proof of Theorem 1

In this section, we first enumerate some properties of mutual information (MI), and then state three easily provable lemmas. Finally, we utilize the properties and lemmas to prove the Theorem 1 stated in Section 3.2.

5.1.1 Properties of MI

For any random variables X , Y and Z :

(P_1) Positivity:

$$I(X; Y) \geq 0, I(X; Y|Z) \geq 0.$$

(P₂) Chain rule:

$$\begin{aligned} I(X, Y; Z) &= I(Y; Z) + I(X; Z|Y) \\ &= I(X; Z) + I(Y; Z|X) \\ &= \frac{1}{2}[I(Y; Z) + I(X; Z) + I(X; Z|Y) + I(Y; Z|X)]. \end{aligned}$$

(P₃) Chain rule (Multivariate Mutual Information):

$$I(X; Y; Z) = I(Y; Z) - I(Y; Z|X).$$

(P₄) Positivity of discrete entropy (for discrete X):

$$H(X) \geq 0, H(X|Y) \geq 0.$$

(P₅) Entropy and Mutual Information:

$$H(X) = H(X|Y) + I(X; Y).$$

5.1.2 Statements of Lemma

Lemma 1 In representation learning, given a random variable X , the random variable Z is defined to be a representation of X , we can simply state that Z is conditionally independent from any other variable in the model once X is observed. That is, for any variable (or groups of variables) T_1 and T_2 in the model, we have

$$I(Z; T_1|X, T_2) = 0.$$

Lemma 2 Given a sequence of random variables X_1, X_2, \dots, X_n and a deterministic function f , then $\forall i, j = 1, 2, \dots, n$, we have

$$I(X_i; f(X_i)) \geq I(X_j; f(X_i)).$$

Proof By the definition,

$$\begin{aligned} I(X_i; f(X_i)) &= H(f(X_i)) - H(f(X_i) | X_i), \\ I(X_j; f(X_i)) &= H(f(X_i)) - H(f(X_i) | X_j). \end{aligned}$$

Since f is a deterministic function,

$$\begin{aligned} H(f(X_i) | X_i) &= 0, \\ H(f(X_i) | X_j) &\geq 0. \end{aligned}$$

Therefore,

$$I(X_i; f(X_i)) \geq I(X_j; f(X_i)).$$

Lemma 3 Let Z_1 and Z_2 are the representation of X_1 and X_2 , respectively, then

$$\begin{aligned} I_\theta(X_1; Z_1|X_2) &\leq D_{\text{KL}}(p_\theta(Z_1|X_1)||p_\psi(Z_2|X_2)), \\ I_\psi(X_2; Z_2|X_1) &\leq D_{\text{KL}}(p_\psi(Z_2|X_2)||p_\theta(Z_1|X_1)). \end{aligned}$$

Proof By the definition,

$$\begin{aligned} I_\theta(X_1; Z_1|X_2) &= \mathbb{E}_{x_1, x_2 \sim p(X_1, X_2)} \mathbb{E}_{z \sim p_\theta(Z_1|X_1)} \left[\log \frac{p_\theta(Z_1 = z|X_1 = x_1)}{p_\theta(Z_1 = z|X_2 = x_2)} \right] \\ &= \mathbb{E}_{x_1, x_2 \sim p(X_1, X_2)} \mathbb{E}_{z \sim p_\theta(Z_1|X_1)} \left[\log \frac{p_\theta(Z_1 = z|X_1 = x_1)}{p_\psi(Z_2 = z|X_2 = x_2)} \right] \\ &\quad - \mathbb{E}_{x_1, x_2 \sim p(X_1, X_2)} \mathbb{E}_{z \sim p_\theta(Z_1|X_1)} \left[\log \frac{p_\theta(Z_1 = z|X_2 = x_2)}{p_\psi(Z_2 = z|X_2 = x_2)} \right] \\ &= D_{\text{KL}}(p_\theta(Z_1|X_1)||p_\psi(Z_2|X_2)) - \\ &\quad D_{\text{KL}}(p_\theta(Z_2|X_1)||p_\psi(Z_2|X_2)) \\ &\leq D_{\text{KL}}(p_\theta(Z_1|X_1)||p_\psi(Z_2|X_2)). \end{aligned}$$

If and only if $p_\psi(Z_2|X_2)$ coincides with $p_\theta(Z_1|X_2)$, the equality holds. Analogously, we can prove $I_\psi(X_2; Z_2|X_1) \leq D_{\text{KL}}(p_\psi(Z_2|X_2)||p_\theta(Z_1|X_1))$.

5.1.3 Proof of Theorem 1

Theorem 1 (Upper Bound of $I(X^v, X^l; T^v, T^l)$) Given two groups of random variables $X = [X^v, X^l]$, $T = [T^v, T^l]$, the mutual information $I(X^v, X^l; T^v, T^l)$ can be upper-bounded with

$$\begin{aligned} I(X; T) &= I(X^v, X^l; T^v, T^l) \\ &\leq \underbrace{I(X^v; T^v)}_{\textcircled{1}} + \underbrace{I(X^l; T^l)}_{\textcircled{2}} - \underbrace{I(T^v; T^l)}_{\textcircled{3}} + \underbrace{D_{\text{SKL}}}_{\textcircled{4}}, \end{aligned} \quad (13)$$

where, D_{SKL} denotes Symmetric Kullback-Leibler (KL) divergence and can be obtained by averaging the divergences $D_{\text{KL}}(p(t^v|x^v)||p(t^l|x^l))$ and $D_{\text{KL}}(p(t^l|x^l)||p(t^v|x^v))$.

Proof

$$\begin{aligned} I(X; T) &= I(X^l, X^v; T) \\ &\stackrel{(P_2)}{=} \frac{1}{2}[I(X^l; T) + I(X^v; T) + I(X^l; T|X^v) \\ &\quad + I(X^v; T|X^l)] \\ &= \frac{1}{2}[I(X^l; T^l, T^v) + I(X^v; T^l, T^v) \\ &\quad + I(X^l; T|X^v) + I(X^v; T|X^l)] \end{aligned}$$

Since,

$$\begin{aligned} I(X^l; T^l, T^v) &\stackrel{(P_2)}{=} I(X^l; T^l) + I(X^l; T^v|T^l) \\ &\stackrel{(P_3)}{=} I(X^l; T^l) + I(X^l; T^v) - I(X^l; T^v; T^l) \\ &\stackrel{(P_3)}{=} I(X^l; T^l) + I(X^l; T^v) - I(T^l; T^v) + I(T^l; T^v|X^l) \\ &\stackrel{(LA1)}{=} I(X^l; T^l) + I(X^l; T^v) - I(T^l; T^v) \\ &\stackrel{(LA2)}{\leq} 2I(X^l; T^l) - I(T^l; T^v). \end{aligned}$$

Analogously, $I(X^v; T^l, T^v)$ is upper bounded by

$$I(X^v; T^l, T^v) \leq 2I(X^v; T^v) - I(T^l; T^v).$$

And,

$$\begin{aligned} I(X^l; T|X^v) &= I(X^l; T^l, T^v|X^v) \\ &\stackrel{(P_2)}{=} I(X^l; T^l|X^v) + I(X^l; T^v|X^v, T^l) \\ &\stackrel{(LA1)}{=} I(X^l; T^l|X^v), \\ I(X^v; T|X^l) &= I(X^v; T^l, T^v|X^l) \\ &\stackrel{(P_2)}{=} I(X^v; T^v|X^l) + I(X^v; T^l|X^l, T^v) \\ &\stackrel{(LA1)}{=} I(X^v; T^v|X^l). \end{aligned}$$

Let $D_{\text{SKL}} = \frac{1}{2}(D_{\text{KL}}(p_\theta||p_\psi) + D_{\text{KL}}(p_\psi||p_\theta))$, therefore,

$$\begin{aligned} I(X; T) &= I(X^l, X^v; T^l, T^v) \\ &\leq I(X^l; T^l) + I(X^v; T^v) - I(T^l; T^v) + \frac{1}{2}[\\ &\quad I(X^l; T^l|X^v) + I(X^v; T^v|X^l)] \\ &\stackrel{(LA3)}{\leq} I(X^l; T^l) + I(X^v; T^v) - I(T^l; T^v) + \frac{1}{2}[\\ &\quad D_{\text{KL}}(p_\theta(T_1|X_1)||p_\psi(T_2|X_2)) + \\ &\quad D_{\text{KL}}(p_\psi(T_2|X_2)||p_\theta(T_1|X_1))] \\ &= I(X^l; T^l) + I(X^v; T^v) - I(T^l; T^v) + D_{\text{SKL}}. \end{aligned}$$

5.2 Proof of Alternative Upper Bound of $I(X^v, X^l; T^v, T^l)$

In this section, we provide the derivations of the meaningful combinations of terms in Eq. (5), i.e., the other three alternative upper bounds of $I(X^v, X^l; T^v, T^l)$ in Section 4.3.1.

$$5.2.1 \quad I(X^l, X^v; T^l, T^v) \leq \frac{3}{2}[I(X^v; T^v) + I(X^l; T^l)]$$

Theorem 3 (Upper Bound of $I(X^v, X^l; T^v, T^l)$) Given two groups of random variables $X = [X^v, X^l]$, $T = [T^v, T^l]$, the mutual information $I(X^v, X^l; T^v, T^l)$ can be upper-bounded with

$$\begin{aligned} I(X; T) &= I(X^v, X^l; T^v, T^l) \\ &\leq \frac{3}{2}[I(X^v; T^v) + I(X^l; T^l)]. \end{aligned} \quad (14)$$

Proof

$$\begin{aligned} I(X; T) &= I(X^l, X^v; T^l, T^v) \\ &\leq I(X^l; T^l) + I(X^v; T^v) - I(T^l; T^v) + \\ &\quad \frac{1}{2}[I(X^l; T^l|X^v) + I(X^v; T^v|X^l)] \\ &\leq I(X^l; T^l) + I(X^v; T^v) + \frac{1}{2}[I(X^l; T^l|X^v) + I(X^v; T^v|X^l)] \\ &\leq I(X^l; T^l) + I(X^v; T^v) + \frac{1}{2}[I(X^l; T^l) + I(X^v; T^v)] \\ &= \frac{3}{2}[I(X^l; T^l) + I(X^v; T^v)]. \end{aligned}$$

$$5.2.2 \quad I(X^l, X^v; T^l, T^v) \leq I(X^v; T^v) + I(X^l; T^l) + D_{\text{SKL}}$$

Theorem 4 (Upper Bound of $I(X^v, X^l; T^v, T^l)$) Given two groups of random variables $X = [X^v, X^l]$, $T = [T^v, T^l]$, the mutual information $I(X^v, X^l; T^v, T^l)$ can be upper-bounded with

$$\begin{aligned} I(X; T) &= I(X^v, X^l; T^v, T^l) \\ &\leq I(X^v; T^v) + I(X^l; T^l) + D_{\text{SKL}}. \end{aligned} \quad (15)$$

where, D_{SKL} denotes the Symmetric Kullback-Leibler (KL) divergence and can be obtained by averaging the divergence $D_{\text{KL}}(p(t^v|x^v)||p(t^l|x^l))$ and $D_{\text{KL}}(p(t^l|x^l)||p(t^v|x^v))$.

Proof

$$\begin{aligned} I(X; T) &= I(X^l, X^v; T^l, T^v) \\ &\stackrel{(\text{Theorem 1})}{\leq} I(X^l; T^l) + I(X^v; T^v) - I(T^l; T^v) + D_{\text{SKL}} \\ &\stackrel{(I(T^l; T^v) \geq 0)}{\leq} I(X^l; T^l) + I(X^v; T^v) + D_{\text{SKL}}. \end{aligned}$$

$$5.2.3 \quad I(X^l, X^v; T^l, T^v) \leq -I(T^v; T^l) + D_{\text{SKL}}$$

Theorem 5 (Upper Bound of $I(X^v, X^l; T^v, T^l)$) Given two groups of random variables $X = [X^v, X^l]$, $T = [T^v, T^l]$, the mutual information $I(X^v, X^l; T^v, T^l)$ can be upper-bounded with

$$\begin{aligned} I(X; T) &= I(X^v, X^l; T^v, T^l) \\ &\leq -I(T^v; T^l) + D_{\text{SKL}}. \end{aligned} \quad (16)$$

where, D_{SKL} denotes the Symmetric Kullback-Leibler (KL) divergence and can be obtained by averaging the divergence $D_{\text{KL}}(p(t^v|x^v)||p(t^l|x^l))$ and $D_{\text{KL}}(p(t^l|x^l)||p(t^v|x^v))$.

Please see the work of Federici et al. (Federici et al., 2020) for proof.

6 Conclusion

In this paper, we propose to improve input robustness when adapting pretrained VLMs to the downstream VQA task from the Information Bottleneck perspective. Specifically, we first derive a new IB lower bound (CIB) for vision-language learning, and then apply CIB to finetune pretrained VLMs with different architectures for VQA. Extensive experiments on five datasets of input robustness consistently demonstrate the effectiveness and superiority of CIB. In the future, we plan to assess the effectiveness of CIB when tuning pretrained VLMs using parameter-effective strategies, such as adapter-based tuning and prompt-based tuning.

Limitation. Redundancy has two sides. One of the reason why pretrained VLMs can significantly improve the performance of the downstream tasks is that they have learned rich and redundant knowledge in the pretraining stage. Practically, for downstream tasks, especially in-domain tasks, task-related redundancy can help models quickly adapt to the new tasks, while task-agnostic redundancy will simultaneously impair model robustness. Our work investigates improving the input robustness of models while preserving their accuracy by seeking a tradeoff between representation compression and redundancy. Another potential study direction is to explore how to explicitly reduce task-agnostic redundancy and adequately exploit task-related redundancy when adapting pretrained VLMs to downstream tasks, especially out-domain tasks.

References

- Antol S, Agrawal A, Lu J, Mitchell M, Batra D, Zitnick CL, Parikh D (2015) Vqa: Visual question answering. In: IEEE Conference on Computer Vision and Pattern Recognition, pp 2425–2433
- Wang W, Bao H, Dong L, Bjorck J, Peng Z, Liu Q, Aggarwal K, Mohammed OK, Singhal S, Som S, et al. (2022) Image as a foreign language: Beit pretraining for all vision and vision-language tasks. arXiv preprint arXiv:220810442
- Zeng Y, Zhang X, Li H, Wang J, Zhang J, Zhou W (2022) X²-VLM: All-in-one pre-trained model for vision-language tasks. arXiv preprint arXiv:221112402
- Wang P, Yang A, Men R, Lin J, Bai S, Li Z, Ma J, Zhou C, Zhou J, Yang H (2022) OFA: Unifying architectures, tasks, and modalities through a simple sequence-to-sequence learning framework. In: International Conference on Machine Learning, pp 23318–23340
- Yu J, Wang Z, Vasudevan V, Yeung L, Seyedhosseini M, Wu Y (2022) Coca: Contrastive captioners are image-text foundation models. arXiv preprint arXiv:220501917
- Wang Z, Yu J, Yu AW, Dai Z, Tsvetkov Y, Cao Y (2022) Simvlm: Simple visual language model pretraining with weak supervision. In: International Conference on Learning Representations
- Li J, Li D, Xiong C, Hoi S (2022) Blip: Bootstrapping language-image pre-training for unified vision-language understanding and generation. arXiv preprint arXiv:220112086
- Yuan L, Chen D, Chen YL, Codella N, Dai X, Gao J, Hu H, Huang X, Li B, Li C, et al. (2021) Florence: A new foundation model for computer vision. arXiv preprint arXiv:211111432
- Wang W, Bao H, Dong L, Wei F (2021) Vlmo: Unified vision-language pre-training with mixture-of-modality-experts. arXiv preprint arXiv:211102358
- Agarwal V, Shetty R, Fritz M (2020) Towards causal vqa: Revealing and reducing spurious correlations by invariant and covariant semantic editing. In: IEEE Conference on Computer Vision and Pattern Recognition, pp 9690–9698
- Shah M, Chen X, Rohrbach M, Parikh D (2019) Cycle-consistency for robust visual question answering. In: IEEE Conference on Computer Vision and Pattern Recognition, pp 6649–6658
- Whitehead S, Wu H, Fung YR, Ji H, Feris R, Saenko K (2020) Learning from lexical perturbations for consistent visual question answering. arXiv preprint arXiv:201113406
- Dancette C, Cadene R, Teney D, Cord M (2021) Beyond question-based biases: Assessing multimodal shortcut learning in visual question answering. In: IEEE International Conference on Computer Vision, pp 1574–1583
- Tishby N, Pereira FC, Bialek W (2000) The information bottleneck method. arXiv preprint physics/0004057
- Li LH, Yatskar M, Yin D, Hsieh CJ, Chang KW (2019) Visualbert: A simple and performant baseline for vision and language. arXiv preprint arXiv:190803557
- Su W, Zhu X, Cao Y, Li B, Lu L, Wei F, Dai J (2020) VL-BERT: pre-training of generic visual-linguistic representations. In: International Conference on Learning Representations
- Chen YC, Li L, Yu L, El Kholy A, Ahmed F, Gan Z, Cheng Y, Liu J (2020) UNITER: Universal image-text representation learning. In: European Conference on Computer Vision, pp 104–120
- Tan H, Bansal M (2019) LXMERT: Learning cross-modality encoder representations from transformers. In: Conference on Empirical Methods in Natural Language Processing, pp 5099–5110
- Lu J, Batra D, Parikh D, Lee S (2019) ViLBERT: pretraining task-agnostic visiolinguistic representations for vision-and-language tasks. In: Neural Information Processing Systems, pp 13–23
- Cho J, Lei J, Tan H, Bansal M (2021) Unifying vision-and-language tasks via text generation. In: International Conference on Machine Learning, pp 1931–1942
- Li J, Selvaraju RR, Gotmare A, Joty SR, Xiong C, Hoi SC (2021) Align before fuse: Vision and language representation learning with momentum distillation. In: Neural Information Processing Systems, pp 9694–9705
- Kant Y, Moudgil A, Batra D, Parikh D, Agrawal H (2021) Contrast and classify: Training robust vqa models. In: IEEE International Conference on Computer Vision, pp 1604–1613
- Li L, Lei J, Gan Z, Liu J (2021) Adversarial vqa: A new benchmark for evaluating the robustness of vqa models. In: IEEE Conference on Computer Vision and Pattern Recognition, pp 2042–2051
- Sheng S, Singh A, Goswami V, Magana JAL, Galuba W, Parikh D, Kiela D (2021) Human-adversarial visual question answering. In: Neural Information Processing Systems, pp 20346–20359
- Agrawal A, Kajić I, Bugliarello E, Davoodi E, Gergely A, Blunsom P, Nematzadeh A (2022) Rethinking evaluation practices in visual question answering: A case study on out-of-distribution generalization. arXiv preprint arXiv:220512191
- Pan Y, Li Z, Zhang L, Tang J (2022) Causal inference with knowledge distilling and curriculum learning for unbiased vqa. ACM Transactions on Multimedia Computing, Communications, and Applications 18(3):1–23
- Kervadec C, Antipov G, Baccouche M, Wolf C (2021) Roses are red, violets are blue... but should vqa expect them to? In: IEEE Conference on Computer Vision and Pattern Recognition, pp 2776–2785
- Jiang J, Liu Z, Liu Y, Nan Z, Zheng N (2021) X-ggm: Graph generative modeling for out-of-distribution generalization in visual question answering. In: ACM International conference on Multimedia, pp 199–208

- Teney D, Kafle K, Shrestha R, Abbasnejad E, Kanan C, Hengel Avd (2020) On the value of out-of-distribution testing: An example of goodhart's law. In: *Neural Information Processing Systems*, pp 407–417
- Clark C, Yatskar M, Zettlemoyer L (2019) Don't take the easy way out: Ensemble based methods for avoiding known dataset biases. In: *Conference on Empirical Methods in Natural Language Processing*, pp 4067–4080
- Goyal Y, Khot T, Summers-Stay D, Batra D, Parikh D (2017) Making the v in vqa matter: Elevating the role of image understanding in visual question answering. In: *IEEE Conference on Computer Vision and Pattern Recognition*, pp 6904–6913
- Li L, Gan Z, Liu J (2020) A closer look at the robustness of vision-and-language pre-trained models. *arXiv preprint arXiv:201208673*
- Tishby N, Zaslavsky N (2015) Deep learning and the information bottleneck principle. In: *IEEE Information Theory Workshop*, pp 1–5
- Shwartz-Ziv R, Tishby N (2017) Opening the black box of deep neural networks via information. *arXiv preprint arXiv:170300810*
- Du Y, Xu J, Xiong H, Qiu Q, Zhen X, Snoek CG, Shao L (2020) Learning to learn with variational information bottleneck for domain generalization. In: *European Conference on Computer Vision*, pp 200–216
- Li B, Shen Y, Wang Y, Zhu W, Li D, Keutzer K, Zhao H (2022) Invariant information bottleneck for domain generalization. In: *Association for the Advancement of Artificial Intelligence*, pp 7399–7407
- Ahuja K, Caballero E, Zhang D, Bengio Y, Mitliagkas I, Rish I (2021) Invariance principle meets information bottleneck for out-of-distribution generalization. In: *Neural Information Processing Systems*, pp 3438–3450
- Federici M, Dutta A, Forré P, Kushman N, Akata Z (2020) Learning robust representations via multi-view information bottleneck. In: *International Conference on Learning Representations*
- Bao F (2021) Disentangled variational information bottleneck for multi-view representation learning. In: *International Conference on Artificial Intelligence*, pp 91–102
- Mahabadi RK, Belinkov Y, Henderson J (2021) Variational information bottleneck for effective low-resource fine-tuning. In: *International Conference on Learning Representations*
- Wang B, Wang S, Cheng Y, Gan Z, Jia R, Li B, Liu J (2021) InfoBERT: Improving robustness of language models from an information theoretic perspective. In: *International Conference on Learning Representations*
- Wang H, Guo X, Deng ZH, Lu Y (2022) Rethinking minimal sufficient representation in contrastive learning. In: *IEEE Conference on Computer Vision and Pattern Recognition*, pp 16041–16050
- Zhou D, Yu Z, Xie E, Xiao C, Anandkumar A, Feng J, Alvarez JM (2022) Understanding the robustness in vision transformers. In: *International Conference on Machine Learning*, pp 27378–27394
- Pan Z, Niu L, Zhang J, Zhang L (2021) Disentangled information bottleneck. In: *Association for the Advancement of Artificial Intelligence*, pp 9285–9293
- Jeon I, Lee W, Pyeon M, Kim G (2021) Ib-gan: Disentangled representation learning with information bottleneck generative adversarial networks. In: *Association for the Advancement of Artificial Intelligence*, pp 7926–7934
- Dubois Y, Kiela D, Schwab DJ, Vedantam R (2020) Learning optimal representations with the decodable information bottleneck. In: *Neural Information Processing Systems*, pp 18674–18690
- Huang Z, Zeng Z, Liu B, Fu D, Fu J (2020) Pixel-BERT: Aligning image pixels with text by deep multi-modal transformers. *arXiv preprint arXiv:200400849*
- Zhou L, Palangi H, Zhang L, Hu H, Corso J, Gao J (2020) Unified vision-language pre-training for image captioning and vqa. In: *Association for the Advancement of Artificial Intelligence*, pp 13041–13049
- Shi L, Shuang K, Geng S, Su P, Jiang Z, Gao P, Fu Z, de Melo G, Su S (2020) Contrastive visual-linguistic pretraining. *arXiv preprint arXiv:200713135*
- Li C, Yan M, Xu H, Luo F, Wang W, Bi B, Huang S (2021) SemVLP: Vision-language pre-training by aligning semantics at multiple levels. *arXiv preprint arXiv:210307829*
- Kim W, Son B, Kim I (2021) Vilt: Vision-and-language transformer without convolution or region supervision. In: *International Conference on Machine Learning*, pp 5583–5594
- Sun S, Chen YC, Li L, Wang S, Fang Y, Liu J (2021) Lightningdot: Pre-training visual-semantic embeddings for real-time image-text retrieval. In: *Annual Meeting of the Association for Computational Linguistics*, pp 982–997
- Huang Z, Zeng Z, Huang Y, Liu B, Fu D, Fu J (2021) Seeing out of the box: End-to-end pre-training for vision-language representation learning. In: *IEEE Conference on Computer Vision and Pattern Recognition*, pp 12976–12985
- Dou ZY, Xu Y, Gan Z, Wang J, Wang S, Wang L, Zhu C, Zhang P, Yuan L, Peng N, et al. (2022) An empirical study of training end-to-end vision-and-language transformers. In: *IEEE Conference on Computer Vision and Pattern Recognition*, pp 18166–18176
- Zhong Y, Yang J, Zhang P, Li C, Codella N, Li LH, Zhou L, Dai X, Yuan L, Li Y, et al. (2022) Regionclip: Region-based language-image pretraining. In: *IEEE Conference on Computer Vision and Pattern Recognition*, pp 16793–16803
- Gan Z, Chen YC, Li L, Zhu C, Cheng Y, Liu J (2020) Large-scale adversarial training for vision-and-language representation learning. In: *Neural Information Processing Systems*, pp 6616–6628
- Li X, Yin X, Li C, Zhang P, Hu X, Zhang L, Wang L, Hu H, Dong L, Wei F, et al. (2020) Oscar: Object-semantics aligned pre-training for vision-language tasks. In: *European Conference on Computer Vision*, pp 121–137
- Zhang P, Li X, Hu X, Yang J, Zhang L, Wang L, Choi Y, Gao J (2021) Vinyl: Revisiting visual representations in vision-language models. In: *IEEE Conference on Computer Vision and Pattern Recognition*, pp 5579–5588
- Lu J, Goswami V, Rohrbach M, Parikh D, Lee S (2020) 12-in-1: Multi-task vision and language representation learning. In: *IEEE Conference on Computer Vision and Pattern Recognition*, pp 10437–10446
- Yu F, Tang J, Yin W, Sun Y, Tian H, Wu H, Wang H (2021) Ernie-vil: Knowledge enhanced vision-language representations through scene graphs. In: *Association for the Advancement of Artificial Intelligence*, pp 3208–3216
- Li Y, Pan Y, Yao T, Chen J, Mei T (2021) Scheduled sampling in vision-language pretraining with decoupled encoder-decoder network. In: *Association for the Advancement of Artificial Intelligence*, pp 8518–8526
- Zeng Y, Zhang X, Li H (2022) Multi-grained vision language pre-training: Aligning texts with visual concepts. In: *International Conference on Machine Learning*, pp 25994–26009
- Vaswani A, Shazeer N, Parmar N, Uszkoreit J, Jones L, Gomez AN, Kaiser Ł, Polosukhin I (2017) Attention is all you need. In: *Neural Information Processing Systems*, pp 5998–6008
- Barber D, Agakov F (2003) The im algorithm: a variational approach to information maximization. In: *Neural Information Processing Systems*, pp 201–208
- Bennasar M, Hicks Y, Setchi R (2015) Feature selection using joint mutual information maximisation. *Expert Systems with Applications* 42(22):8520–8532
- Cheng P, Hao W, Dai S, Liu J, Gan Z, Carin L (2020) CLUB: A contrastive log-ratio upper bound of mutual information. In: *International Conference on Machine Learning*, pp 1779–1788
- Poole B, Ozair S, Van Den Oord A, Alemi A, Tucker G (2019) On variational bounds of mutual information. In: *International Conference on Machine Learning*, pp 5171–5180
- Anderson P, He X, Buehler C, Teney D, Johnson M, Gould S, Zhang L (2018) Bottom-up and top-down attention for image captioning and visual question answering. In: *IEEE Conference on Computer*

- Vision and Pattern Recognition, pp 6077–6086
- Jiang Y, Natarajan V, Chen X, Rohrbach M, Batra D, Parikh D (2018) Pythia v0. 1: the winning entry to the vqa challenge 2018. arXiv preprint arXiv:180709956
- Kim JH, Jun J, Zhang BT (2018) Bilinear attention networks. In: Neural Information Processing Systems, pp 1564–1574
- Chen X, Fang H, Lin TY, Vedantam R, Gupta S, Dollár P, Zitnick CL (2015) Microsoft coco captions: Data collection and evaluation server. arXiv preprint arXiv:150400325
- Krishna R, Zhu Y, Groth O, Johnson J, Hata K, Kravitz J, Chen S, Kalantidis Y, Li LJ, Shamma DA, et al. (2017) Visual Genome: Connecting language and vision using crowdsourced dense image annotations. *International Journal of Computer Vision* 123(1):32–73
- Hudson DA, Manning CD (2019) Gqa: A new dataset for real-world visual reasoning and compositional question answering. In: IEEE Conference on Computer Vision and Pattern Recognition, pp 6700–6709
- Zhu Y, Groth O, Bernstein M, Fei-Fei L (2016) Visual7w: Grounded question answering in images. In: IEEE Conference on Computer Vision and Pattern Recognition, pp 4995–5004
- Sharma P, Ding N, Goodman S, Soricut R (2018) Conceptual captions: A cleaned, hypernymed, image alt-text dataset for automatic image captioning. In: Annual Meeting of the Association for Computational Linguistics, pp 2556–2565
- Ordonez V, Kulkarni G, Berg T (2011) Im2text: Describing images using 1 million captioned photographs. In: Neural Information Processing Systems, pp 1143–1151
- Hu R, Andreas J, Darrell T, Saenko K (2018) Explainable neural computation via stack neural module networks. In: European Conference on Computer Vision, pp 53–69
- Shi J, Zhang H, Li J (2019) Explainable and explicit visual reasoning over scene graphs. In: IEEE Conference on Computer Vision and Pattern Recognition, pp 8376–8384
- Lu J, Lin X, Batra D, Parikh D (2015) Deeper lstm and normalized cnn visual question answering model. https://github.com/VT-vision-lab/VQA_LSTM_CNN
- Kazemi V, Elqursh A (2017) Show, ask, attend, and answer: A strong baseline for visual question answering. arXiv preprint arXiv:170403162
- Yang Z, He X, Gao J, Deng L, Smola A (2016) Stacked attention networks for image question answering. In: IEEE Conference on Computer Vision and Pattern Recognition, pp 21–29
- Ben-Younes H, Cadene R, Thome N, Cord M (2019) Block: Bilinear superdiagonal fusion for visual question answering and visual relationship detection. In: Association for the Advancement of Artificial Intelligence, pp 8102–8109
- Cadene R, Dancette C, Cord M, Parikh D, et al. (2019) RUBi: Reducing unimodal biases for visual question answering. In: Neural Information Processing Systems, pp 841–852
- Gat I, Schwartz I, Schwing A, Hazan T (2020) Removing bias in multimodal classifiers: Regularization by maximizing functional entropies. In: Neural Information Processing Systems, pp 3197–3208
- Shrestha R, Kafle K, Kanan C (2020) A negative case analysis of visual grounding methods for vqa. In: Annual Meeting of the Association for Computational Linguistics, pp 8172–8181
- Nam J, Cha H, Ahn SS, Lee J, Shin J (2020) Learning from failure: De-biasing classifier from biased classifier. In: Neural Information Processing Systems, pp 20673–20684
- Chen L, Yan X, Xiao J, Zhang H, Pu S, Zhuang Y (2020) Counterfactual samples synthesizing for robust visual question answering. In: IEEE Conference on Computer Vision and Pattern Recognition, pp 10800–10809
- Oord Avd, Li Y, Vinyals O (2018) Representation learning with contrastive predictive coding. arXiv preprint arXiv:180703748
- Nguyen X, Wainwright MJ, Jordan MI (2010) Estimating divergence functionals and the likelihood ratio by convex risk minimization. *IEEE Transactions on Information Theory* 56(11):5847–5861
- Belghazi MI, Baratin A, Rajeswar S, Ozair S, Bengio Y, Courville A, Hjelm RD (2018) Mutual information neural estimation. In: International Conference on Machine Learning, pp 530–539
- Yu L, Poirson P, Yang S, Berg AC, Berg TL (2016) Modeling context in referring expressions. In: European Conference on Computer Vision, pp 69–85
- Liu X, Li L, Wang S, Zha ZJ, Meng D, Huang Q (2019) Adaptive reconstruction network for weakly supervised referring expression grounding. In: IEEE International Conference on Computer Vision, pp 2611–2620
- Zhang Z, Zhao Z, Lin Z, He X, et al. (2020) Counterfactual contrastive learning for weakly-supervised vision-language grounding. In: Neural Information Processing Systems, pp 18123–18134